Contents lists available at ScienceDirect

Physics Letters B

PHYSICS LETTERS B

CrossMark

Freeze-out radii extracted from three-pion cumulants in pp, p–Pb and Pb–Pb collisions at the LHC

ALICE Collaboration [*]

ABSTRACT

In high-energy collisions, the spatio-temporal size of the particle production region can be measured using the Bose–Einstein correlations of identical bosons at low relative momentum. The source radii are typically extracted using two-pion correlations, and characterize the system at the last stage of interaction, called kinetic freeze-out. In low-multiplicity collisions, unlike in high-multiplicity collisions, two-pion correlations are substantially altered by background correlations, e.g. mini-jets. Such correlations can be suppressed using three-pion cumulant correlations. We present the first measurements of the size of the system at freeze-out extracted from three-pion cumulant correlations in pp, p–Pb and Pb–Pb collisions at the LHC with ALICE. At similar multiplicity, the invariant radii extracted in p–Pb collisions are found to be 5–15% larger than those in pp, while those in Pb–Pb are 35–55% larger than those in p–Pb. Our measurements disfavor models which incorporate substantially stronger collective expansion in p–Pb as compared to pp collisions at similar multiplicity.

© 2014 The Authors. Published by Elsevier B.V. This is an open access article under the CC BY license (http://creativecommons.org/licenses/by/3.0/). Funded by SCOAP³.

1. Introduction

The role of initial and final-state effects in interpreting differences between Pb–Pb and pp collisions is expected to be clarified with p–Pb collisions [1]. However, the results obtained from p–Pb collisions at $\sqrt{s_{NN}} = 5.02$ TeV [2–10] have not been conclusive since they can be explained assuming either a hydrodynamic phase during the evolution of the system [11–13] or the formation of a Color Glass Condensate (CGC) in the initial state [14,15].

As in Pb–Pb collisions, the presence of a hydrodynamic phase in high-multiplicity p–Pb collisions is expected to lead to a factor of 1.5–2 larger freeze-out radii than in pp collisions at similar multiplicity [16]. In contrast, a CGC initial state model (IP-Glasma), without a hydrodynamic phase, predicts similar freeze-out radii in p–Pb and pp collisions [17]. A measurement of the freeze-out radii in the two systems will thus lead to additional experimental constraints on the interpretation of the p–Pb data.

The extraction of freeze-out radii can be achieved using identical boson correlations at low relative momentum, which are dominated by quantum statistics (QS) and final-state Coulomb and strong interactions (FSIs). Both FSIs and QS correlations encode information about the femtoscopic space–time structure of the particle emitting source at kinetic freeze-out [18–20]. The calculation of FSI correlations allows for the isolation of QS correlations.

Typically, two-pion QS correlations are used to extract the characteristic radius of the source [21–27]. However, higher-order QS correlations can be used as well [28–32]. The novel features of higher-order QS correlations are extracted using the cumulant for which all lower order correlations are removed [33,34]. The maximum of the three-pion cumulant QS correlation is a factor of two larger than for two-pion QS correlations [33–36]. In addition to the increased signal, three-pion cumulants also remove contributions from two-particle background correlations unrelated to QS (e.g. from mini-jets [24,26]). The combined effect of an increased signal and decreased background is advantageous in low multiplicity systems where a substantial background exists.

In this Letter, we present measurements of freeze-out radii extracted using three-pion cumulant QS correlations. The invariant radii are extracted in intervals of multiplicity and triplet momentum in pp ($\sqrt{s} = 7$ TeV), p–Pb ($\sqrt{s_{NN}} = 5.02$ TeV) and Pb–Pb ($\sqrt{s_{NN}} = 2.76$ TeV) which allows for a comparison of the various systems. The radii extracted from three-pion cumulants are also compared to those from two-pion correlations.

The Letter is organized into 5 remaining sections. Section 2 explains the experimental setup and event selection. Section 3 describes the identification of pions, as well as the measurement of the event multiplicity. Section 4 explains the three-pion cumulant analysis technique used to extract the source radii. Section 5 presents the measured source radii. Finally, Section 6 summarizes the results reported in the Letter.

[*] *E-mail address:* alice-publications@cern.ch.

2. Experimental setup and event selection

Data from pp, p–Pb, and Pb–Pb collisions at the LHC recorded with ALICE [37] are analyzed. The data for pp collisions were taken during the 2010 pp run at $\sqrt{s} = 7$ TeV, for p–Pb collisions during the 2013 run at $\sqrt{s_{NN}} = 5.02$ TeV, and for Pb–Pb during the 2010 and 2011 runs at $\sqrt{s_{NN}} = 2.76$ TeV. For p–Pb, the proton beam energy was 4 TeV while for the lead beam it was 1.58 TeV per nucleon. Thus, the nucleon–nucleon center-of-mass system moved with respect to the ALICE laboratory system with a rapidity of -0.465, i.e. in the direction of the proton beam. The pseudorapidity in the laboratory system is denoted with η throughout this Letter, which for the pp and Pb–Pb systems coincides with the pseudorapidity in the center-of-mass system.

The trigger conditions are slightly different for each of the three collision systems. For pp collisions, the VZERO detectors [38] located in the forward and backward regions of the detector, as well as the Silicon Pixel Detector (SPD) at mid-rapidity are used to form a minimum-bias trigger by requiring at least one hit in the SPD or either of the VZERO detectors [39]. For Pb–Pb and p–Pb collisions, the trigger is formed by requiring simultaneous hits in both VZERO detectors. In addition, high-multiplicity triggers in pp and p–Pb collisions based on the SPD are used. Two additional triggers in Pb–Pb are used based on the VZERO signal amplitude which enhanced the statistics for central and semi-central collisions [38]. Approximately 164, 115, and 52 million events are used for pp, p–Pb, and Pb–Pb collisions, respectively. For pp and p–Pb, the high multiplicity triggers account for less than 3% of the collected events. For Pb–Pb, the central and semi-central triggers account for about 40% and 52% of the collected events, respectively.

The Inner Tracking System (ITS) and Time Projection Chamber (TPC) located at mid-rapidity are used for particle tracking [40]. The ITS consists of 6 layers of silicon detectors: silicon pixel (layers 1, 2), silicon drift (layers 3, 4), and silicon strip (layers 5, 6) detectors. The ITS provides high spatial resolution of the primary vertex. The TPC alone is used for momentum and charge determination of particles via their curvature in the 0.5 T longitudinal magnetic field, since cluster sharing within the ITS causes a small momentum bias for particle pairs at low relative momentum.

The TPC additionally provides particle identification capabilities through the specific ionization energy loss (dE/dx). The Time Of Flight (TOF) detector is also used to select particles at higher momenta. To ensure uniform tracking, the z-coordinate (beam-axis) of the primary vertex is required to be within a distance of 10 cm from the detector center. Events with less than three reconstructed charged pions are rejected, which removes about 25% and 10% of the low-multiplicity events in pp and p–Pb, respectively.

3. Track selection and multiplicity intervals

Tracks with total momentum less than 1.0 GeV/c are used to ensure good particle identification. We also require transverse momentum $p_T > 0.16$ GeV/c, and pseudorapidity $|\eta| < 0.8$. To ensure good momentum resolution a minimum of 70 tracking points in the TPC are required. Charged pions are selected if they are within 2 standard deviations (σ) of the expected pion dE/dx value [41]. For momenta greater than 0.6 GeV/c, high purity is maintained with TOF by selecting particles within 2σ of the expected pion time-of-flight. Additionally, tracks which are within 2σ of the expected kaon or proton dE/dx or time-of-flight values are rejected. The effects of track merging and splitting are minimized based on the spatial separation of tracks in the TPC as described in [42]. For three-pion correlations the pair cuts are applied to each of the three pairs in the triplet.

Similar as in [10], the analysis is performed in intervals of multiplicity which are defined by the reconstructed number of charged pions, N_{pions}^{rec}, in the above-mentioned kinematic range. For each multiplicity interval, the corresponding mean acceptance and efficiency corrected value of the total charged-pion multiplicity, $\langle N_{pions} \rangle$, and the total charged-particle multiplicity, $\langle N_{ch} \rangle$, are determined using detector simulations with PYTHIA [43], DPM-JET [44], and HIJING [45] event generators. The systematic uncertainty of $\langle N_{ch} \rangle$ and $\langle N_{pions} \rangle$ is determined by comparing PYTHIA to PHOJET (pp) [46], DPMJET to HIJING (p–Pb), and HIJING to AMPT (Pb–Pb) [47], and amounts to about 5%. The multiplicity intervals, $\langle N_{pions} \rangle$, $\langle N_{ch} \rangle$, as well as the average centrality in Pb–Pb and fractional cross sections in pp and p–Pb are given in Table 1. The collision centrality in Pb–Pb is determined using the charged-particle multiplicity in the VZERO detectors [38]. As mentioned above, the center-of-mass reference frame for p–Pb collisions does not coincide with the laboratory frame, where $\langle N_{ch} \rangle$ is measured. However, from studies using DPMJET and HIJING at the generator level, the difference to $\langle N_{ch} \rangle$ measured in the center-of-mass is expected to be smaller than 3%.

4. Analysis technique

To extract the source radii, one can measure two- and three-particle correlation functions as in Ref. [42]. The two-particle correlation function

$$C_2(p_1, p_2) = \alpha_2 \frac{N_2(p_1, p_2)}{N_1(p_1)N_1(p_2)} \qquad (1)$$

is constructed using the momenta p_i, and is defined as the ratio of the inclusive two-particle spectrum over the product of the inclusive single-particle spectra. Both are projected onto the Lorentz invariant relative momentum $q = \sqrt{-(p_1 - p_2)^\mu (p_1 - p_2)_\mu}$ and the average pion transverse momentum $k_T = |\vec{p}_{T,1} + \vec{p}_{T,2}|/2$. The numerator of the correlation function is formed by all pairs of particles from the same event. The denominator is formed by taking one particle from one event and the second particle from another event within the same multiplicity interval. The normalization factor, α_2, is determined such that the correlation function equals unity in a certain interval of relative momentum q. The location of the interval is sufficiently above the dominant region of QS+FSI correlations and sufficiently narrow to avoid the influence of non-femtoscopic correlations at large relative momentum. As the width of QS+FSI correlations is different in all three collision systems, our choice for the normalization interval depends on the multiplicity interval. For Pb–Pb, the normalization intervals are $0.15 < q < 0.175$ GeV/c for $N_{pions}^{rec} \geq 400$ and $0.3 < q < 0.35$ GeV/c for $N_{pions}^{rec} < 400$. For pp and p–Pb the normalization interval is $1.0 < q < 1.2$ GeV/c.

Following [48,49], the two-particle QS distributions, N_2^{QS}, and correlations, C_2^{QS}, are extracted from the measured distributions in intervals of k_T assuming

$$C_2(q) = \mathcal{N}\left[(1 - f_c^2) + f_c^2 K_2(q) C_2^{QS}(q) \right] B(q). \qquad (2)$$

The parameter f_c^2 characterizes the combined dilution effect of weak decays and long-lived resonance decays in the "core/halo" picture [50,51]. In Pb–Pb, it was estimated to be 0.7 ± 0.05 with mixed-charge two-pion correlations [42]. The same procedure performed in pp and p–Pb data results in compatible values. The FSI correlation is given by $K_2(q)$, which includes Coulomb and strong interactions. For low multiplicities ($N_{pions}^{rec} < 150$), $K_2(q)$ is calculated iteratively using the Fourier transform of the FSI corrected correlation functions. For higher multiplicities ($N_{pions}^{rec} \geq 150$), $K_2(q)$ is calculated as in Ref. [42] using the THERMINATOR2

Table 1

Multiplicity intervals as determined by the reconstructed number of charged pions, $N_{\text{pions}}^{\text{rec}}$, with all of the track selection cuts ($p < 1.0$ GeV/c, $p_{\text{T}} > 0.16$ GeV/c, $|\eta| < 0.8$). $\langle N_{\text{pions}}\rangle$ stands for the acceptance corrected average number of charged pions, and $\langle N_{\text{ch}}\rangle$ for corresponding acceptance corrected number of charged particles in the same kinematic range. The uncertainties on $\langle N_{\text{ch}}\rangle$ are about 5%. The RMS width of the $\langle N_{\text{ch}}\rangle$ distribution in each interval ranges from 10% to 35% for the highest and lowest multiplicity intervals, respectively. The average centrality for Pb–Pb in percentiles, as well as the fractional cross-sections of the multiplicity intervals for p–Pb and pp are also given. The RMS widths for the centralities range from about 2 to 4 percentiles for central and peripheral collisions, respectively.

$N_{\text{pions}}^{\text{rec}}$	Pb–Pb data			p–Pb data			pp data		
	$\langle$Cent$\rangle$	$\langle N_{\text{pions}}\rangle$	$\langle N_{\text{ch}}\rangle$	Fraction	$\langle N_{\text{pions}}\rangle$	$\langle N_{\text{ch}}\rangle$	Fraction	$\langle N_{\text{pions}}\rangle$	$\langle N_{\text{ch}}\rangle$
[3, 5)	–	–	–	0.10	–	–	0.23	4.0	4.6
[5, 10)	–	–	–	0.20	8.5	9.8	0.31	7.7	8.6
[10, 15)	–	–	–	0.18	15	17	0.12	13	15
[15, 20)	–	–	–	0.14	20	23	0.05	18	20
[20, 30)	77%	26	36	0.17	29	33	0.03	24	27
[30, 40)	73%	37	50	0.07	40	45	0.003	34	37
[40, 50)	70%	49	64	0.03	51	57	1×10^{-4}	44	47
[50, 70)	66%	66	84	0.01	63	71	–	–	–
[70, 100)	60%	95	118	–	–	–	–	–	–
[100, 150)	53%	142	172	–	–	–	–	–	–
[150, 200)	48%	213	253	–	–	–	–	–	–
[200, 260)	43%	276	326	–	–	–	–	–	–
[260, 320)	38%	343	403	–	–	–	–	–	–
[320, 400)	33%	426	498	–	–	–	–	–	–
[400, 500)	28%	534	622	–	–	–	–	–	–
[500, 600)	22%	654	760	–	–	–	–	–	–
[600, 700)	18%	777	901	–	–	–	–	–	–
[700, 850)	13%	931	1076	–	–	–	–	–	–
[850, 1050)	7.4%	1225	1413	–	–	–	–	–	–
[1050, 2000)	2.6%	1590	1830	–	–	–	–	–	–

model [52,53]. $B(q)$ represents the non-femtoscopic background correlation, and is taken from PYTHIA and DPMJET for pp and p–Pb, respectively [24,26]. It is set equal to unity for Pb–Pb, where no significant background is expected. In Eq. (2), $\mathcal{N}$ is the residual normalization of the fit which typically differs from unity by 0.01.

The same-charge two-pion QS correlation can be parametrized by an exponential

$$C_2^{\text{QS}}(q) = 1 + \lambda e^{-R_{\text{inv}}q}, \tag{3}$$

as well as by a Gaussian or Edgeworth expansion

$$C_2^{\text{QS}}(q) = 1 + \lambda E_{\text{w}}^2(R_{\text{inv}}q)e^{-R_{\text{inv}}^2 q^2} \tag{4}$$

$$E_{\text{w}}(R_{\text{inv}}q) = 1 + \sum_{n=3}^{\infty}\frac{\kappa_n}{n!(\sqrt{2})^n}H_n(R_{\text{inv}}q), \tag{5}$$

where $E_{\text{w}}(R_{\text{inv}}q)$ characterizes deviations from Gaussian behavior, H_n are the Hermite polynomials, and κ_n are the Edgeworth coefficients [54]. The first two relevant Edgeworth coefficients (κ_3, κ_4) are found to be sufficient to describe the non-Gaussian features at low relative momentum. The Gaussian functional form is obtained with $E_{\text{w}} = 1$ ($\kappa_n = 0$) in Eq. (4). The parameter λ characterizes an apparent suppression from an incorrectly assumed functional form of C_2^{QS} and the suppression due to possible pion coherence [55]. The parameter R_{inv} is the characteristic radius from two-particle correlations evaluated in the pair-rest frame. The effective intercept parameter for the Edgeworth fit is given by $\lambda_{\text{e}} = \lambda E_{\text{w}}^2(0)$ [54]. The effective intercept can be below the chaotic limit of 1.0 for partially coherent emission [36,42,55]. The extracted effective intercept parameter is found to strongly depend on the assumed functional form of C_2^{QS}.

The three-particle correlation function

$$C_3(p_1, p_2, p_3) = \alpha_3 \frac{N_3(p_1, p_2, p_3)}{N_1(p_1)N_1(p_2)N_1(p_3)} \tag{6}$$

is defined as the ratio of the inclusive three-particle spectrum over the product of the inclusive single-particle spectra. In analogy to the two-pion case, it is projected onto the Lorentz invariant $Q_3 = \sqrt{q_{12}^2 + q_{31}^2 + q_{23}^2}$ and the average pion transverse mo-

mentum $K_{\text{T},3} = \frac{|\vec{p}_{\text{T},1}+\vec{p}_{\text{T},2}+\vec{p}_{\text{T},3}|}{3}$. The numerator of C_3 is formed by taking three particles from the same event. The denominator is formed by taking each of the three particles from different events. The normalization factor, α_3, is determined such that the correlation function equals unity in the interval of Q_3 where each pair q_{ij} lies in the same interval given before for two-pion correlations.

The extraction of the full three-pion QS distribution, N_3^{QS}, in intervals of $K_{\text{T},3}$ is done as in Ref. [42] by measuring

$$N_3(p_1, p_2, p_3) = f_1 N_1(p_1)N_1(p_2)N_1(p_3)$$
$$+ f_2\big[N_2(p_1, p_2)N_1(p_3) + N_2(p_3, p_1)N_1(p_2)$$
$$+ N_2(p_2, p_3)N_1(p_1)\big]$$
$$+ f_3 K_3(q_{12}, q_{31}, q_{23})N_3^{\text{QS}}(p_1, p_2, p_3), \tag{7}$$

where the fractions $f_1 = (1 - f_c)^3 + 3f_c(1 - f_c)^2 - 3(1 - f_c)(1 - f_c^2) = -0.08$, $f_2 = 1 - f_c = 0.16$, and $f_3 = f_c^3 = 0.59$ using $f_c^2 = 0.7$ as in the two-pion case. The term $N_2(p_i, p_j)N_1(p_k)$ is formed by taking two particles from the same event and the third particle from a mixed event. All three-particle distributions are normalized to each other in the same way as for α_3. $K_3(q_{12}, q_{31}, q_{23})$ denotes the three-pion FSI correlation, which in the generalized Riverside (GRS) approach [42,56,57] is approximated by $K_2(q_{12})K_2(q_{31})K_2(q_{23})$. It was found to describe the $\pi^\pm\pi^\pm\pi^\mp$ three-body FSI correlation to the few percent level [42]. From Eq. (7) one can extract N_3^{QS} and construct the three-pion QS cumulant correlation

$$\mathbf{c}_3(p_1, p_2, p_3) = \mathcal{N}_3\big[1 + [2N_1(p_1)N_1(p_2)N_1(p_3)$$
$$- N_2^{\text{QS}}(p_1, p_2)N_1(p_3)$$
$$- N_2^{\text{QS}}(p_3, p_1)N_1(p_2) - N_2^{\text{QS}}(p_2, p_3)N_1(p_1)$$
$$+ N_3^{\text{QS}}(p_1, p_2, p_3)]/N_1(p_1)N_1(p_2)N_1(p_3)\big], \tag{8}$$

where $N_2^{\text{QS}}(p_i, p_j)N_1(p_k) = [N_2(p_i, p_j)N_1(p_k) - N_1(p_i)N_1(p_j) \times N_1(p_k)(1 - f_c^2)]/(f_c^2 K_2)$. In Eq. (8), all two-pion QS correlations are explicitly subtracted [34]. The QS cumulant in this form has
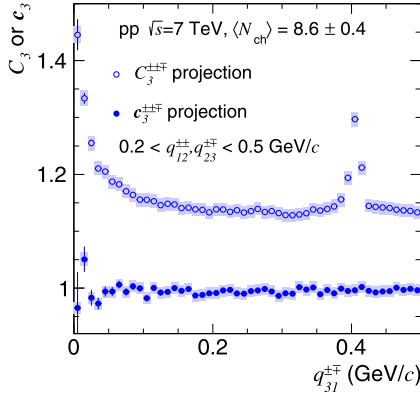
Fig. 1. Demonstration of the removal of the K_s^0 decay from three-pion cumulants. Mixed-charge three-pion correlations are projected against the relative momentum of a mixed-charge pair ($q_{31}^{\pm\mp}$). The K_s^0 decay into a $\pi^+ + \pi^-$ pair is visible as expected around 0.4 GeV/c. The FSI enhancement of the mixed-charge pair "31" is also visible at low $q_{31}^{\pm\mp}$. FSI corrections are not applied. Systematic uncertainties are shown by shaded boxes.

FSIs removed before its construction. $\mathcal{N}_3$ is the residual normalization of the fit which typically differs from unity by 0.02.

The three-pion same-charge cumulant correlations are then projected onto 3D pair relative momenta and fit with an exponential

$$\mathbf{c}_3(q_{12}, q_{31}, q_{23}) = 1 + \lambda_3 e^{-R_{\mathrm{inv},3}(q_{12}+q_{31}+q_{23})/2}, \qquad (9)$$

as well as a Gaussian and an Edgeworth expansion [54]

$$\mathbf{c}_3(q_{12}, q_{31}, q_{23}) = 1 + \lambda_3 E_{\mathrm{w}}(R_{\mathrm{inv},3} q_{12}) E_{\mathrm{w}}(R_{\mathrm{inv},3} q_{31})$$
$$\times E_{\mathrm{w}}(R_{\mathrm{inv},3} q_{23}) e^{-R_{\mathrm{inv},3}^2 Q_3^2/2}. \qquad (10)$$

$R_{\mathrm{inv},3}$ and λ_3 are the invariant radius and intercept parameters extracted from three-pion cumulant correlations, respectively. The effective intercept parameter for the Edgeworth fit is $\lambda_{\mathrm{e},3} = \lambda_3 E_{\mathrm{w}}^3(0)$. For an exact functional form of $\mathbf{c}_3$, $\lambda_{\mathrm{e},3}$ reaches a maximum of 2.0 for fully chaotic pion emission. Deviations below and above 2.0 can further be caused by incorrect representations of $\mathbf{c}_3$, e.g. Gaussian. Eq. (10) neglects the effect of the three-pion phase [33] which was found to be consistent with zero for Pb–Pb central and midcentral collisions [42]. We note that the extracted radii from two- and three-pion correlations need not exactly agree, e.g. in the case of coherent emission [58].

The measured correlation functions need to be corrected for finite track momentum resolution of the TPC which causes a slight broadening of the correlation functions and leads to a slight decrease of the extracted radii. PYTHIA (pp), DPMJET (p–Pb) and HIJING (Pb–Pb) simulations are used to estimate the effect on the fit parameters. After the correction, both fit parameters increase by about 2% (5%) for the lowest (highest) multiplicity interval. The relative systematic uncertainty of this correction is conservatively taken to be 1%. The pion purity is estimated to be about 96%. Muons are found to be the dominant source of contamination, for which we apply corrections to the correlation functions as described in Ref. [42]. The correction typically increases the radius (intercept) fit parameters by less than 1% (5%). The corresponding systematic uncertainty is included in the comparison of the mixed-charged correlation with unity (see below).

5. Results

The absence of two-particle correlations in the three-pion cumulant can be demonstrated via the removal of known two-body effects such as the decay of K_s^0 into a $\pi^+ + \pi^-$ pair (Fig. 1).

The mixed-charge three-pion correlation function ($C_3^{\pm\pm\mp}$) projected onto the invariant relative momentum of one of the mixed-charge pairs in the triplet exhibits the K_s^0 peak as expected around $q^{\pm\mp} = 0.4$ GeV/c, while it is removed in the cumulant.

In Fig. 2 we present three-pion correlation functions for same-charge (top panels) and mixed-charge (bottom panels) triplets in pp, p–Pb, and Pb–Pb collision systems in three sample multiplicity intervals. For same-charge triplets, the three-pion cumulant QS correlation ($\mathbf{c}_3^{\pm\pm\pm}$) is clearly visible. For mixed-charge triplets the three-pion cumulant correlation function ($\mathbf{c}_3^{\pm\pm\mp}$) is consistent with unity, as expected when FSIs are removed. Gaussian, Edgeworth, and exponential fits are performed in three dimensions (q_{12}, q_{31}, q_{23}). Concerning Edgeworth fits, different values of the κ coefficients correspond to different spatial freeze-out profiles. In order to make a meaningful comparison of the characteristic radii across all multiplicity intervals and collision systems, we fix $\kappa_3 = 0.1$ and $\kappa_4 = 0.5$. The values are determined from the average of free fits to $\mathbf{c}_3^{\pm\pm\pm}$ for all multiplicity intervals, $K_{\mathrm{T},3}$ intervals and systems. The RMS of both κ_3 and κ_4 distributions is 0.1. The chosen κ coefficients produce a sharper correlation function which corresponds to larger tails in the source distribution. Also shown in Fig. 2 are model calculations of $\mathbf{c}_3$ in PYTHIA (pp), DPMJET (p–Pb) and HIJING (Pb–Pb), which do not contain QS+FSI correlations and demonstrate that three-pion cumulants, in contrast to two-pion correlations [24,26], do not contain a significant non-femtoscopic background, even for low multiplicities.

The systematic uncertainties on C_3 are conservatively estimated to be 1% by comparing π^+ to π^- correlation functions and by tightening the track merging and splitting cuts. The systematic uncertainty on $\mathbf{c}_3^{\pm\pm\pm}$ is estimated by the residual correlation observed with $\mathbf{c}_3^{\pm\pm\mp}$ relative to unity. The residual correlation leads to a 4% uncertainty on $\lambda_{\mathrm{e},3}$ while having a negligible effect on $R_{\mathrm{inv},3}$. The uncertainty on f_c leads to an additional 10% uncertainty on $\mathbf{c}_3 - 1$ and $\lambda_{\mathrm{e},3}$. We also investigated the effect of setting $f_c = 1$ and thus $f_1 = 0$, $f_2 = 0$, $f_3 = 1.0$ in Eq. (7) and found a negligible effect on $R_{\mathrm{inv},3}$, while significantly reducing $\lambda_{\mathrm{e},3}$ as expected when the dilution is not adequately taken into account.

Figs. 3(a) and 3(b) show the three-pion Gaussian fit parameters for low and high $K_{\mathrm{T},3}$ intervals, respectively. The $\langle k_{\mathrm{T}} \rangle$ values for low (high) k_{T} are 0.25 (0.43) GeV/c. The resulting pair k_{T} distributions in the triplet $K_{\mathrm{T},3}$ intervals have RMS widths for the low (high) $K_{\mathrm{T},3}$ of 0.12 (0.14) in pp and p–Pb and 0.04 (0.09) GeV/c in Pb–Pb collisions. The $\langle k_{\mathrm{T}} \rangle$ values for low (high) $K_{\mathrm{T},3}$ are 0.24 (0.39) GeV/c. We also show the fit parameters extracted from two-pion correlations in order to compare to those extracted from three-pion cumulants. For Pb–Pb, the Gaussian radii extracted from three-pion correlations are about 10% smaller than those extracted from two-pion correlations, which may be due to the non-Gaussian features of the correlation function. A clear suppression below the chaotic limit is observed for the effective intercept parameters in all multiplicity intervals. The suppression may be caused by non-Gaussian features of the correlation function and also by a finite coherent component of pion emission [36,42,55].

The systematic uncertainties on the fit parameters are dominated by fit-range variations, especially in the case of Gaussian fits to non-Gaussian correlation functions. The chosen fit range for $\mathbf{c}_3$ varies smoothly between $Q_3 = 0.5$ and 0.1 GeV/c from the lowest multiplicity pp to the highest multiplicity Pb–Pb intervals. For C_2, the fit ranges are chosen to be $\sqrt{2}$ times narrower. The characteristic width of Gaussian three-pion cumulant QS correlations projected against Q_3 is a factor of $\sqrt{2}$ times that of Gaussian two-pion QS correlations projected against q [35,36]. As a variation we change the upper bound of the fit range by $\pm 30\%$ for three-pion correlations and two-pion correlations in Pb–Pb for $N_{\mathrm{pions}}^{\mathrm{rec}} > 50$. For $N_{\mathrm{pions}}^{\mathrm{rec}} < 50$, in Pb–Pb, the upper limit of the fit
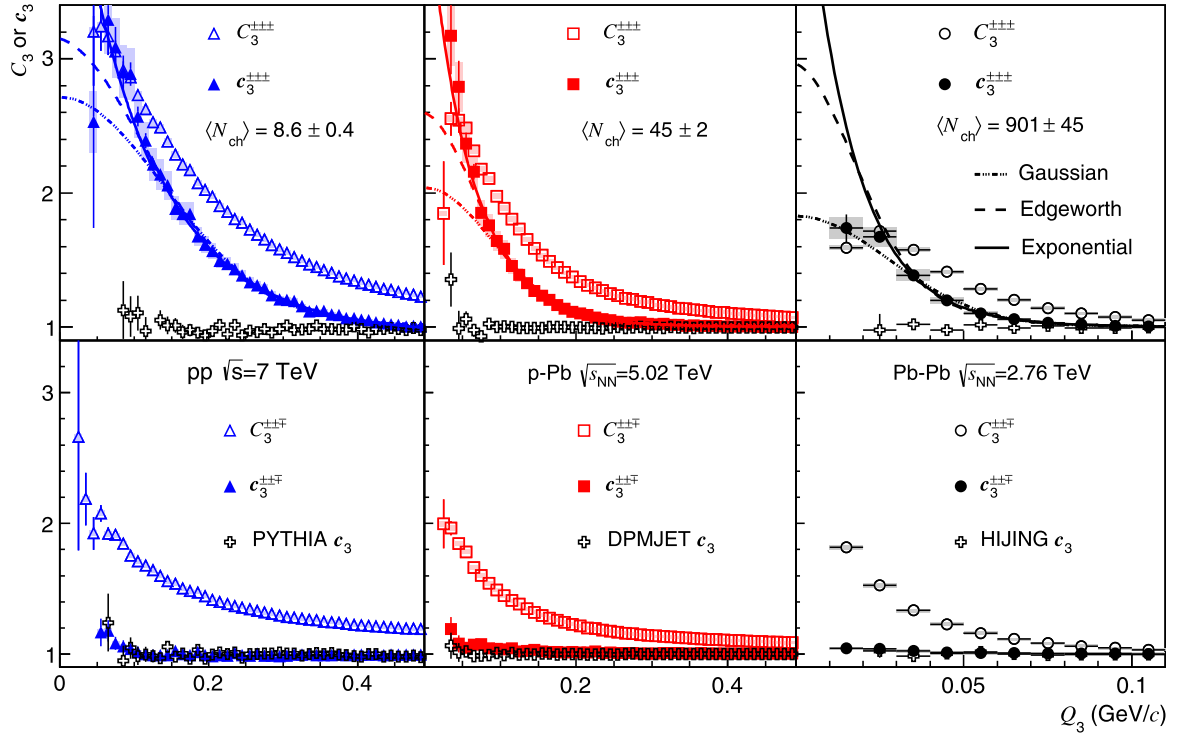
Fig. 2. Three-pion correlation functions versus Q_3 for $0.16 < K_{T,3} < 0.3$ GeV/c in pp, p–Pb and Pb–Pb collision data compared to PYTHIA, DPMJET and HIJING generator-level calculations. Top panels are for same-charge triplets, while bottom panels are for mixed-charge triplets. Two points at low Q_3 with large statistical uncertainties are not shown for the pp same-charge correlation function.
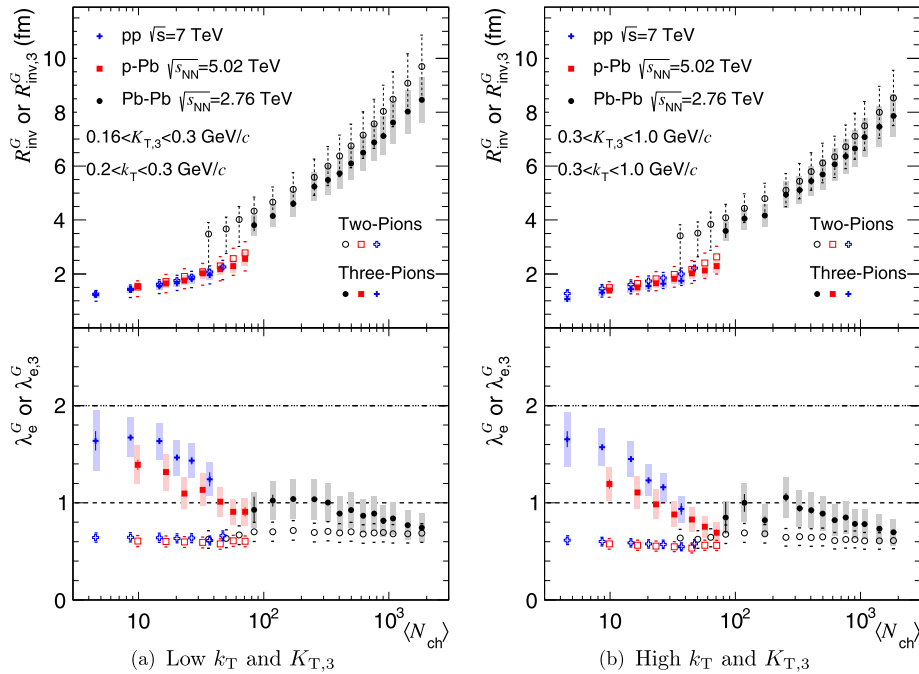

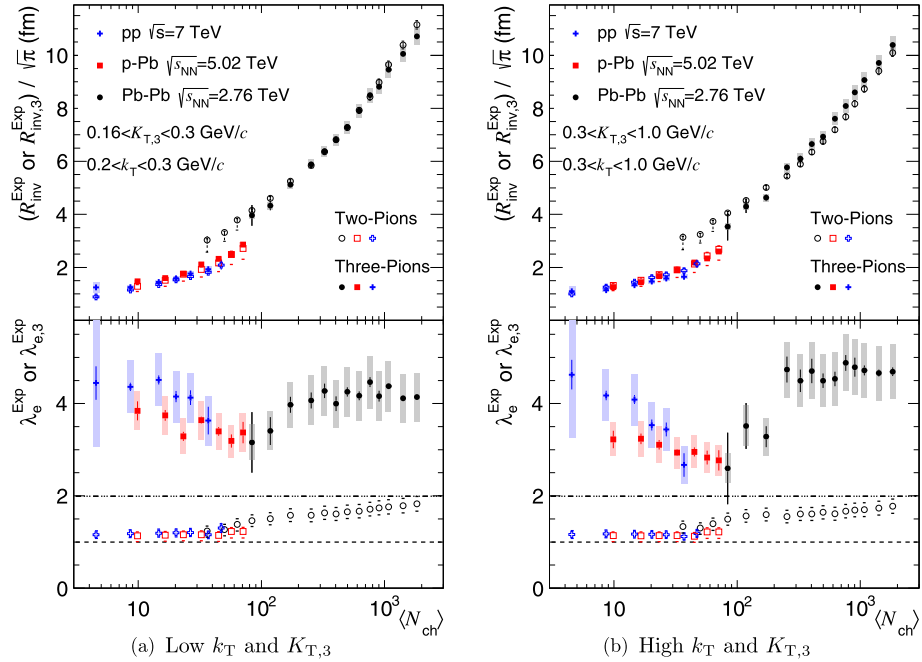**Fig. 3.** Two- and three-pion Gaussian fit parameters versus $\langle N_{ch} \rangle$ in pp, p–Pb and Pb–Pb collision systems for low and high k_T and $K_{T,3}$ intervals. Top panels show the Gaussian radii R_{inv}^G and $R_{inv,3}^G$ and bottom panels show the effective Gaussian intercept parameters λ_e^G and $\lambda_{e,3}^G$. The systematic uncertainties are dominated by fit range variations and are shown by bounding/dashed lines and shaded boxes for two- and three-particle parameters, respectively. The dashed and dash-dotted lines represent the chaotic limits for λ_e^G and $\lambda_{e,3}^G$, respectively.

range is increased to match that in p–Pb (i.e. 0.13 to 0.27 GeV/c). For pp and p–Pb, owing to the larger background present for two-pion correlations, we extend the fit range to $q = 1.2$ GeV/c for the upper variation. The non-femtoscopic background in Eq. (2) has a non-negligible effect on the extracted radii in the extended fit

range. The resulting systematic uncertainties are fully correlated for three-pion fit parameters for each collision system, since the fit-range variations have the same effect in each multiplicity interval. The systematic uncertainties for the two-pion fit parameters are largely correlated and are asymmetric due to the different

Fig. 4. Two- and three-pion Edgeworth fit parameters versus $\langle N_{ch} \rangle$ in pp, p–Pb and Pb–Pb collision systems for low and high k_T and $K_{T,3}$ intervals. Top panels show the Edgeworth radii $R_{inv}^{E_w}$ and $R_{inv,3}^{E_w}$ and bottom panels show the effective intercept parameters $\lambda_e^{E_w}$ and $\lambda_{e,3}^{E_w}$. As described in the text, κ_3 and κ_4 are fixed to 0.1 and 0.5, respectively. Same details as for Fig. 3.

Fig. 5. Two- and three-pion exponential fit parameters versus $\langle N_{ch} \rangle$ in pp, p–Pb and Pb–Pb collision systems for low and high k_T and $K_{T,3}$ intervals. Top panels show the exponential radii R_{inv}^{Exp} and $R_{inv,3}^{Exp}$ scaled down by $\sqrt{\pi}$ and bottom panels show the effective intercept parameters λ_e^{Exp} and $\lambda_{e,3}^{Exp}$. Same details as for Fig. 3.

fit-range variations. We note that the radii in pp collisions at $\sqrt{s} = 7$ TeV from our previous two-pion measurement [26] are about 25% smaller than the central values extracted in this analysis although compatible within systematic uncertainties. The large difference is attributed to the narrower fit range in this analysis. In [24,26] the chosen Gaussian fit range was $q < 1.4$ GeV/c, while here it is $q < 0.35$ GeV/c for the lowest multiplicity interval. The narrower fit range is chosen based on observations made with three-pion cumulants for which two-pion background correlations are removed. It is observed in Fig. 2 that even for low multiplic-

ities, the dominant QS correlation is well below $Q_3 = 0.5$ GeV/c. The presence of the non-femtoscopic backgrounds can also bias the radii from two-pion correlations in wide fit ranges and is suppressed with three-pion cumulant correlations.

To further address the non-Gaussian features of the correlation functions, we also extract the fit parameters from an Edgeworth and exponential parametrization as shown in Figs. 4 and 5. We observe that the Edgeworth and exponential radii are significantly larger than the Gaussian radii. However, they should not be directly compared as they correspond to different source profiles.

Gaussian radii correspond to the standard deviation of a Gaussian source profile whereas exponential radii correspond to the FWHM of a Cauchy source. The Edgeworth radii are model independent and are defined as the 2nd cumulant of the measured correlation function. Note that the exponential radii have been scaled down by $\sqrt{\pi}$ as is often done to compare Gaussian and exponential radii [23]. Compared to the Gaussian radii, the two- and three-pion radii are in much better agreement for the Edgeworth and exponential fits. This suggests that the discrepancy between two- and three-pion Gaussian radii are indeed caused by non-Gaussian features of the correlation function. Concerning the effective intercepts, we observe a substantial increase as compared to the Gaussian case.

The qualities of the Gaussian, Edgeworth, and exponential fits for three-pion cumulant correlations vary depending on the multiplicity interval. The χ^2/NDF for the 3D three-pion Gaussian, Edgeworth, and exponential fits in the highest multiplicity Pb–Pb interval is 8600/1436, 4450/1436, and 4030/1436, respectively. The χ^2/NDF decreases significantly for lower multiplicity intervals to about 4170/7785 for peripheral Pb–Pb and 12 400/17 305 for pp and p–Pb multiplicity intervals, for all fit types. The Edgeworth χ^2/NDF is a few percent smaller than for Gaussian fits in low multiplicity intervals. The exponential χ^2/NDF is a few percent smaller than for Edgeworth fits in low multiplicity intervals.

Due to the asymmetry of the p–Pb colliding system, the extracted fit parameters in $-0.8 < \eta < -0.4$ and $0.4 < \eta < 0.8$ pseudorapidity intervals are compared. The radii and the effective intercept parameters in both intervals are consistent within statistical uncertainties.

The extracted radii in each multiplicity interval and system correspond to different $\langle N_{\text{ch}} \rangle$ values. To compare the radii in pp and p–Pb at the same $\langle N_{\text{ch}} \rangle$ value, we perform a linear fit to the pp three-pion Edgeworth radii as a function of $\langle N_{\text{ch}} \rangle^{1/3}$. We then compare the extracted p–Pb three-pion Edgeworth radii to the value of the pp fit evaluated at the same $\langle N_{\text{ch}} \rangle$. We find that the Edgeworth radii in p–Pb are on average $10 \pm 5\%$ larger than for pp in the region of overlapping multiplicity. The comparison of Pb–Pb to p–Pb radii is done similarly where the fit is performed to p–Pb data and compared to the two-pion Pb–Pb Edgeworth radii. The Edgeworth radii in Pb–Pb are found to be on average $45 \pm 10\%$ larger than for p–Pb in the region of overlapping multiplicity. The ratio comparison as it is done exploits the cancellation of the largely correlated systematic uncertainties.

To be independent of the assumed functional form for $\mathbf{c}_3$, the same-charge three-pion cumulant correlation functions are directly compared between two collision systems at similar multiplicity. Fig. 6(a) shows that while the three-pion correlation functions in pp and p–Pb collisions are different, their characteristic widths are similar. It is therefore the $\lambda_{e,3}$ values which differ the most between the two systems. Fig. 6(b) shows that the correlation functions in p–Pb and Pb–Pb collisions are generally quite different.

6. Summary

Three-pion correlations of same- and mixed-charge pions have been presented for pp ($\sqrt{s} = 7$ TeV), p–Pb ($\sqrt{s_{NN}} = 5.02$ TeV) and Pb–Pb ($\sqrt{s_{NN}} = 2.76$ TeV) collisions at the LHC, measured with ALICE. Freeze-out radii using Gaussian, Edgeworth, and exponential fits have been extracted from the three-pion cumulant QS correlation and presented in intervals of multiplicity and triplet momentum. Compared to the radii from two-pion correlations, the radii from three-pion cumulant correlations are less susceptible to non-femtoscopic background correlations due to the increased QS signal and the removal of two-pion backgrounds.

The deviation of Gaussian fits below the observed correlations at low Q_3 clearly demonstrates the importance of non-Gaussian features of the correlation functions. The effective intercept parameters from Gaussian (exponential) fits are significantly below (above) the chaotic limits, while the corresponding Edgeworth effective intercepts are much closer to the chaotic limit.

At similar multiplicity, the invariant radii extracted from Edgeworth fits in p–Pb collisions are found to be 5–15% larger than those in pp, while those in Pb–Pb are 35–55% larger than those in p–Pb. Hence, models which incorporate substantially stronger collective expansion in p–Pb than pp collisions at similar multiplicity are disfavored. The comparability of the extracted radii in pp and p–Pb collisions at similar multiplicity is consistent with expectations from CGC initial conditions (IP-Glasma) without a hydrodynamic phase [17]. The smaller radii in p–Pb as compared to Pb–Pb collisions may demonstrate the importance of different initial conditions on the final-state, or indicate significant collective expansion already in peripheral Pb–Pb collisions.

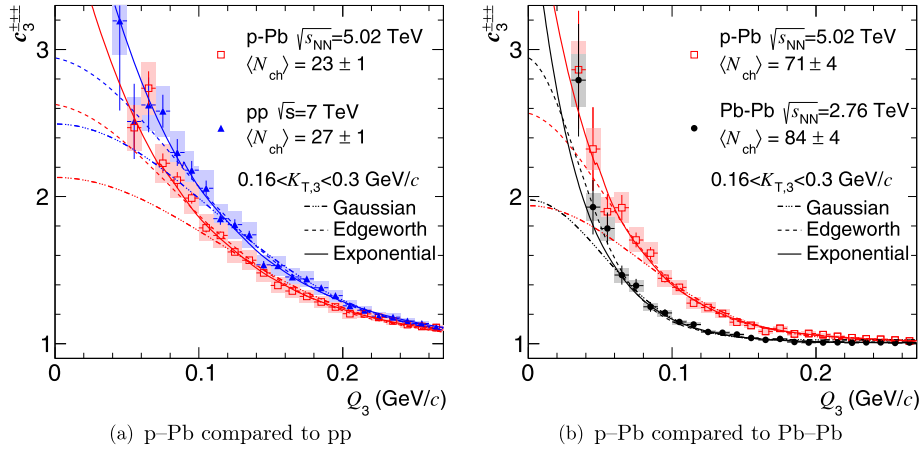(a) p–Pb compared to pp   (b) p–Pb compared to Pb–Pb

Fig. 6. Comparisons of same-charge three-pion cumulant correlation functions at similar multiplicity for $0.16 < K_{T,3} < 0.3$ GeV/c. Three points at low Q_3 with large statistical uncertainties are not shown in the left panel.

References

[1] C. Salgado, et al., J. Phys. G 39 (2012) 015010, arXiv:1105.3919.
[2] CMS Collaboration, S. Chatrchyan, et al., Phys. Lett. B 718 (2013) 795, arXiv:1210.5482.
[3] ALICE Collaboration, B. Abelev, et al., Phys. Lett. B 719 (2013) 29, arXiv:1212.2001.
[4] ATLAS Collaboration, G. Aad, et al., Phys. Rev. Lett. 110 (2013) 182302, arXiv:1212.5198.
[5] ATLAS Collaboration, G. Aad, et al., Phys. Lett. B 725 (2013) 60, arXiv:1303.2084.
[6] CMS Collaboration, S. Chatrchyan, et al., Phys. Lett. B 719 (2013) 29, arXiv:1305.0609.
[7] CMS Collaboration, S. Chatrchyan, et al., arXiv:1307.3442, 2013.
[8] ALICE Collaboration, B. Abelev, et al., Phys. Lett. B 728 (2014) 25, arXiv:1307.6796.
[9] ALICE Collaboration, B. Abelev, et al., Phys. Lett. B 726 (2013) 164, arXiv:1307.3237.
[10] ALICE Collaboration, B. Abelev, et al., Phys. Lett. B 727 (2013) 371, arXiv:1307.1094.
[11] P. Bozek, W. Broniowski, Phys. Lett. B 718 (2013) 1557, arXiv:1211.0845.
[12] P. Bozek, W. Broniowski, Phys. Rev. C 88 (2013) 014903, arXiv:1304.3044.
[13] G.Y. Qin, B. Müller, arXiv:1306.3439, 2013.
[14] K. Dusling, R. Venugopalan, Phys. Rev. D 87 (2013) 054014, arXiv:1211.3701.
[15] K. Dusling, R. Venugopalan, Phys. Rev. D 87 (2013) 094034, arXiv:1302.7018.
[16] P. Bozek, W. Broniowski, Phys. Lett. B 720 (2013) 250, arXiv:1301.3314.
[17] A. Bzdak, et al., Phys. Rev. C 87 (2013) 064906, arXiv:1304.3403.
[18] G. Goldhaber, et al., Phys. Rev. 120 (1960) 300.
[19] G. Kopylov, M. Podgoretsky, Zh. Eksp. Teor. Fiz. 69 (1975) 414.
[20] R. Lednicky, Phys. Part. Nucl. 40 (2009) 307, arXiv:nucl-th/0501065.
[21] STAR Collaboration, J. Adams, et al., Phys. Rev. C 71 (2005) 044906, arXiv:nucl-ex/0411036.
[22] M.A. Lisa, et al., Annu. Rev. Nucl. Part. Sci. 55 (2005) 357, arXiv:nucl-ex/0505014.
[23] CMS Collaboration, V. Khachatryan, et al., Phys. Rev. Lett. 105 (2010) 032001, arXiv:1005.3294.
[24] ALICE Collaboration, K. Aamodt, et al., Phys. Rev. D 82 (2010) 052001, arXiv:1007.0516.

[25] CMS Collaboration, V. Khachatryan, et al., J. High Energy Phys. 1105 (2011) 029, arXiv:1101.3518.
[26] ALICE Collaboration, K. Aamodt, et al., Phys. Rev. D 84 (2011) 112004, arXiv:1101.3665.
[27] ALICE Collaboration, K. Aamodt, et al., Phys. Lett. B 696 (2011) 328, arXiv:1012.4035.
[28] UA1-Minimum Bias-Collaboration, N. Neumeister, et al., Phys. Lett. B 275 (1992) 186.
[29] NA44 Collaboration, I. Bearden, et al., Phys. Lett. B 517 (2001) 25, arXiv:nucl-ex/0102013.
[30] OPAL Collaboration, K. Ackerstaff, et al., Eur. Phys. J. C 5 (1998) 239, arXiv:hep-ex/9806036.
[31] DELPHI Collaboration, P. Abreu, et al., Phys. Lett. B 355 (1995) 415.
[32] L3 Collaboration, P. Achard, et al., Phys. Lett. B 540 (2002) 185, arXiv:hep-ex/0206051.
[33] U.W. Heinz, Q. Zhang, Phys. Rev. C 56 (1997) 426, arXiv:nucl-th/9701023.
[34] U.W. Heinz, A. Sugarbaker, Phys. Rev. C 70 (2004) 054908, arXiv:nucl-th/0408056.
[35] R. Weiner, Phys. Lett. B 232 (1989) 278.
[36] I. Andreev, M. Plumer, R. Weiner, Int. J. Mod. Phys. A 8 (1993) 4577.
[37] ALICE Collaboration, K. Aamodt, et al., J. Instrum. 3 (2008) S08002.
[38] ALICE Collaboration, B. Abelev, et al., Phys. Rev. C 88 (2013) 044909, arXiv:1301.4361.
[39] ALICE Collaboration, K. Aamodt, et al., Phys. Rev. Lett. 105 (2010) 252301, arXiv:1011.3916.
[40] J. Alme, et al., Nucl. Instrum. Methods Phys. Res., Sect. A, Accel. Spectrom. Detect. Assoc. Equip. 622 (2010) 316, arXiv:1001.1950.
[41] ALICE Collaboration, B. Abelev, et al., arXiv:1402.4476, 2014.
[42] ALICE Collaboration, B. Abelev, et al., Phys. Rev. C 89 (2014) 024911, arXiv:1310.7808.
[43] T. Sjostrand, S. Mrenna, P.Z. Skands, J. High Energy Phys. 0605 (2006) 026, arXiv:hep-ph/0603175.
[44] S. Roesler, R. Engel, J. Ranft, SLAC-PUB-8740, p. 1033, arXiv:hep-ph/0012252, 2000.
[45] X.N. Wang, M. Gyulassy, Phys. Rev. D 44 (1991) 3501.
[46] R. Engel, Z. Phys. C 66 (1995) 203.
[47] Z.W. Lin, et al., Phys. Rev. C 72 (2005) 064901, arXiv:nucl-th/0411110.
[48] M. Bowler, Phys. Lett. B 270 (1991) 69.
[49] Y. Sinyukov, et al., Phys. Lett. B 432 (1998) 248.
[50] R. Lednicky, M. Podgoretsky, Sov. J. Nucl. Phys. 30 (1979) 432.
[51] T. Csorgo, B. Lorstad, J. Zimanyi, Z. Phys. C 71 (1996) 491, arXiv:hep-ph/9411307.
[52] A. Kisiel, et al., Comput. Phys. Commun. 174 (2006) 669, arXiv:nucl-th/0504047.
[53] M. Chojnacki, et al., Comput. Phys. Commun. 183 (2012) 746, arXiv:1102.0273.
[54] T. Csorgo, S. Hegyi, Phys. Lett. B 489 (2000) 15.
[55] S. Akkelin, R. Lednicky, Y. Sinyukov, Phys. Rev. C 65 (2002) 064904, arXiv:nucl-th/0107015.
[56] WA98 Collaboration, M. Aggarwal, et al., Phys. Rev. Lett. 85 (2000) 2895, arXiv:hep-ex/0008018.
[57] STAR Collaboration, J. Adams, et al., Phys. Rev. Lett. 91 (2003) 262301, arXiv:nucl-ex/0306028.
[58] M. Plumer, L. Razumov, R. Weiner, Phys. Lett. B 286 (1992) 335.

ALICE Collaboration

B. Abelev [bq], J. Adam [ak], D. Adamová [by], M.M. Aggarwal [cc], M. Agnello [da,cj], A. Agostinelli [z], N. Agrawal [ar], Z. Ahammed [dt], N. Ahmad [r], I. Ahmed [o], S.U. Ahn [bj], S.A. Ahn [bj], I. Aimo [da,cj], S. Aiola [dy], M. Ajaz [o], A. Akindinov [ba], S.N. Alam [dt], D. Aleksandrov [cp], B. Alessandro [da], D. Alexandre [cr], A. Alici [l,cu], A. Alkin [c], J. Alme [ai], T. Alt [am], S. Altinpinar [q], I. Altsybeev [ds], C. Alves Garcia Prado [di], C. Andrei [bt], A. Andronic [cm], V. Anguelov [ci], J. Anielski [aw], T. Antičić [cn], F. Antinori [cx], P. Antonioli [cu], L. Aphecetche [dc], H. Appelshäuser [av], N. Arbor [bm], S. Arcelli [z], N. Armesto [p], R. Arnaldi [da], T. Aronsson [dy], I.C. Arsene [cm], M. Arslandok [av], A. Augustinus [ah], R. Averbeck [cm], T.C. Awes [bz], M.D. Azmi [ce], M. Bach [am], A. Badalà [cw], Y.W. Baek [bl,an], S. Bagnasco [da], R. Bailhache [av], R. Bala [cf], A. Baldisseri [n], F. Baltasar Dos Santos Pedrosa [ah], R.C. Baral [bd], R. Barbera [aa], F. Barile [ae], G.G. Barnaföldi [dx], L.S. Barnby [cr], V. Barret [bl], J. Bartke [df], M. Basile [z], N. Bastid [bl], S. Basu [dt], B. Bathen [aw], G. Batigne [dc], B. Batyunya [bi], P.C. Batzing [u], C. Baumann [av], I.G. Bearden [bv], H. Beck [av], C. Bedda [cj], N.K. Behera [ar], I. Belikov [ax], F. Bellini [z], R. Bellwied [dk], E. Belmont-Moreno [bg], R. Belmont [dw], V. Belyaev [br], G. Bencedi [dx], S. Beole [y], I. Berceanu [bt], A. Bercuci [bt], Y. Berdnikov [ca,i], D. Berenyi [dx], M.E. Berger [ch], R.A. Bertens [az], D. Berzano [y], L. Betev [ah], A. Bhasin [cf], I.R. Bhat [cf], A.K. Bhati [cc], B. Bhattacharjee [ao], J. Bhom [dp], L. Bianchi [y], N. Bianchi [bn], C. Bianchin [az], J. Bielčík [ak], J. Bielčíková [by], A. Bilandzic [bv], S. Bjelogrlic [az], F. Blanco [j], D. Blau [cp], C. Blume [av], F. Bock [ci,bp], A. Bogdanov [br], H. Bøggild [bv], M. Bogolyubsky [db], F.V. Böhmer [ch], L. Boldizsár [dx], M. Bombara [al], J. Book [av], H. Borel [n], A. Borissov [cl,dw], F. Bossú [bh], M. Botje [bw], E. Botta [y], S. Böttger [au], P. Braun-Munzinger [cm], M. Bregant [di], T. Breitner [au], T.A. Broker [av], T.A. Browning [ck], M. Broz [ak], E. Bruna [da], G.E. Bruno [ae], D. Budnikov [co], H. Buesching [av], S. Bufalino [da], P. Buncic [ah], O. Busch [ci], Z. Buthelezi [bh], D. Caffarri [ab], X. Cai [g], H. Caines [dy], L. Calero Diaz [bn], A. Caliva [az], E. Calvo Villar [cs], P. Camerini [x], F. Carena [ah], W. Carena [ah], J. Castillo Castellanos [n], E.A.R. Casula [w], V. Catanescu [bt], C. Cavicchioli [ah], C. Ceballos Sanchez [i], J. Cepila [ak], P. Cerello [da], B. Chang [dl], S. Chapeland [ah], J.L. Charvet [n], S. Chattopadhyay [dt], S. Chattopadhyay [cq], V. Chelnokov [c], M. Cherney [cb], C. Cheshkov [dr], B. Cheynis [dr], V. Chibante Barroso [ah], D.D. Chinellato [dk], P. Chochula [ah], M. Chojnacki [bv], S. Choudhury [dt], P. Christakoglou [bw], C.H. Christensen [bv], P. Christiansen [af], T. Chujo [dp], S.U. Chung [cl], C. Cicalo [cv], L. Cifarelli [l,z], F. Cindolo [cu], J. Cleymans [ce], F. Colamaria [ae], D. Colella [ae], A. Collu [w], M. Colocci [z], G. Conesa Balbastre [bm], Z. Conesa del Valle [at], M.E. Connors [dy], J.G. Contreras [k], T.M. Cormier [dw], Y. Corrales Morales [y], P. Cortese [ad], I. Cortés Maldonado [b], M.R. Cosentino [di], F. Costa [ah], P. Crochet [bl], R. Cruz Albino [k], E. Cuautle [bf], L. Cunqueiro [bn], A. Dainese [cx], R. Dang [g], A. Danu [be], D. Das [cq], I. Das [at], K. Das [cq], S. Das [d], A. Dash [dj], S. Dash [ar], S. De [dt], H. Delagrange [dc,ii], A. Deloff [bs], E. Dénes [dx], G. D'Erasmo [ae], A. De Caro [ac,l], G. de Cataldo [ct], J. de Cuveland [am], A. De Falco [w], D. De Gruttola [ac,l], N. De Marco [da], S. De Pasquale [ac], R. de Rooij [az], M.A. Diaz Corchero [j], T. Dietel [aw], P. Dillenseger [av], R. Divià [ah], D. Di Bari [ae], S. Di Liberto [cy], A. Di Mauro [ah], P. Di Nezza [bn], Ø. Djuvsland [q], A. Dobrin [az], T. Dobrowolski [bs], D. Domenicis Gimenez [di], B. Dönigus [av], O. Dordic [u], S. Dørheim [ch], A.K. Dubey [dt], A. Dubla [az], L. Ducroux [dr], P. Dupieux [bl], A.K. Dutta Majumdar [cq], R.J. Ehlers [dy], D. Elia [ct], H. Engel [au], B. Erazmus [ah,dc], H.A. Erdal [ai], D. Eschweiler [am], B. Espagnon [at], M. Esposito [ah], M. Estienne [dc], S. Esumi [dp], D. Evans [cr], S. Evdokimov [db], D. Fabris [cx], J. Faivre [bm], D. Falchieri [z], A. Fantoni [bn], M. Fasel [ci], D. Fehlker [q], L. Feldkamp [aw], D. Felea [be], A. Feliciello [da], G. Feofilov [ds], J. Ferencei [by], A. Fernández Téllez [b], E.G. Ferreiro [p], A. Ferretti [y], A. Festanti [ab], J. Figiel [df], M.A.S. Figueredo [dm], S. Filchagin [co], D. Finogeev [ay], F.M. Fionda [ae], E.M. Fiore [ae], E. Floratos [cd], M. Floris [ah], S. Foertsch [bh], P. Foka [cm], S. Fokin [cp], E. Fragiacomo [cz], A. Francescon [ah,ab], U. Frankenfeld [cm], U. Fuchs [ah], C. Furget [bm], M. Fusco Girard [ac], J.J. Gaardhøje [bv], M. Gagliardi [y], A.M. Gago [cs], M. Gallio [y], D.R. Gangadharan [bp,s], P. Ganoti [bz], C. Garabatos [cm], E. Garcia-Solis [m], C. Gargiulo [ah], I. Garishvili [bq], J. Gerhard [am], M. Germain [dc], A. Gheata [ah], M. Gheata [ah,be], B. Ghidini [ae], P. Ghosh [dt], S.K. Ghosh [d], P. Gianotti [bn], P. Giubellino [ah], E. Gladysz-Dziadus [df], P. Glässel [ci], A. Gomez Ramirez [au], P. González-Zamora [j], S. Gorbunov [am], L. Görlich [df], S. Gotovac [de], L.K. Graczykowski [dv], A. Grelli [az], A. Grigoras [ah], C. Grigoras [ah], V. Grigoriev [br], A. Grigoryan [a], S. Grigoryan [bi], B. Grinyov [c], N. Grion [cz], J.F. Grosse-Oetringhaus [ah], J.-Y. Grossiord [dr], R. Grosso [ah], F. Guber [ay], R. Guernane [bm], B. Guerzoni [z], M. Guilbaud [dr], K. Gulbrandsen [bv], H. Gulkanyan [a], M. Gumbo [ce], T. Gunji [do], A. Gupta [cf], R. Gupta [cf], K.H. Khan [o], R. Haake [aw], Ø. Haaland [q], C. Hadjidakis [at], M. Haiduc [be], H. Hamagaki [do], G. Hamar [dx], L.D. Hanratty [cr], A. Hansen [bv], J.W. Harris [dy], H. Hartmann [am], A. Harton [m], D. Hatzifotiadou [cu], S. Hayashi [do], S.T. Heckel [av], M. Heide [aw], H. Helstrup [ai], A. Herghelegiu [bt],

G. Herrera Corral [k], B.A. Hess [ag], K.F. Hetland [ai], B. Hippolyte [ax], J. Hladky [bc], P. Hristov [ah], M. Huang [q], T.J. Humanic [s], D. Hutter [am], D.S. Hwang [t], R. Ilkaev [co], I. Ilkiv [bs], M. Inaba [dp], G.M. Innocenti [y], C. Ionita [ah], M. Ippolitov [cp], M. Irfan [r], M. Ivanov [cm], V. Ivanov [ca], A. Jachołkowski [aa], P.M. Jacobs [bp], C. Jahnke [di], H.J. Jang [bj], M.A. Janik [dv], P.H.S.Y. Jayarathna [dk], S. Jena [dk], R.T. Jimenez Bustamante [bf], P.G. Jones [cr], H. Jung [an], A. Jusko [cr], V. Kadyshevskiy [bi], S. Kalcher [am], P. Kalinak [bb], A. Kalweit [ah], J. Kamin [av], J.H. Kang [dz], V. Kaplin [br], S. Kar [dt], A. Karasu Uysal [bk], O. Karavichev [ay], T. Karavicheva [ay], E. Karpechev [ay], U. Kebschull [au], R. Keidel [ea], M.M. Khan [r,iii], P. Khan [cq], S.A. Khan [dt], A. Khanzadeev [ca], Y. Kharlov [db], B. Kileng [ai], B. Kim [dz], D.W. Kim [bj,an], D.J. Kim [dl], J.S. Kim [an], M. Kim [an], M. Kim [dz], S. Kim [t], T. Kim [dz], S. Kirsch [am], I. Kisel [am], S. Kiselev [ba], A. Kisiel [dv], G. Kiss [dx], J.L. Klay [f], J. Klein [ci], C. Klein-Bösing [aw], A. Kluge [ah], M.L. Knichel [cm], A.G. Knospe [dg], C. Kobdaj [ah,dd], M.K. Köhler [cm], T. Kollegger [am], A. Kolojvari [ds], V. Kondratiev [ds], N. Kondratyeva [br], A. Konevskikh [ay], V. Kovalenko [ds], M. Kowalski [df], S. Kox [bm], G. Koyithatta Meethaleveedu [ar], J. Kral [dl], I. Králik [bb], F. Kramer [av], A. Kravčáková [al], M. Krelina [ak], M. Kretz [am], M. Krivda [cr,bb], F. Krizek [by], E. Kryshen [ah], M. Krzewicki [cm], V. Kučera [by], Y. Kucheriaev [cp,ii], T. Kugathasan [ah], C. Kuhn [ax], P.G. Kuijer [bw], I. Kulakov [av], J. Kumar [ar], P. Kurashvili [bs], A. Kurepin [ay], A.B. Kurepin [ay], A. Kuryakin [co], S. Kushpil [by], M.J. Kweon [ci], Y. Kwon [dz], P. Ladron de Guevara [bf], C. Lagana Fernandes [di], I. Lakomov [at], R. Langoy [du], C. Lara [au], A. Lardeux [dc], A. Lattuca [y], S.L. La Pointe [az], P. La Rocca [aa], R. Lea [x], G.R. Lee [cr], I. Legrand [ah], J. Lehnert [av], R.C. Lemmon [bx], V. Lenti [ct], E. Leogrande [az], M. Leoncino [y], I. León Monzón [dh], P. Lévai [dx], S. Li [g,bl], J. Lien [du], R. Lietava [cr], S. Lindal [u], V. Lindenstruth [am], C. Lippmann [cm], M.A. Lisa [s], H.M. Ljunggren [af], D.F. Lodato [az], P.I. Loenne [q], V.R. Loggins [dw], V. Loginov [br], D. Lohner [ci], C. Loizides [bp], X. Lopez [bl], E. López Torres [i], X.-G. Lu [ci], P. Luettig [av], M. Lunardon [ab], G. Luparello [az], C. Luzzi [ah], R. Ma [dy], A. Maevskaya [ay], M. Mager [ah], D.P. Mahapatra [bd], S.M. Mahmood [u], A. Maire [ci], R.D. Majka [dy], M. Malaev [ca], I. Maldonado Cervantes [bf], L. Malinina [bi,iv], D. Mal'Kevich [ba], P. Malzacher [cm], A. Mamonov [co], L. Manceau [da], V. Manko [cp], F. Manso [bl], V. Manzari [ct], M. Marchisone [bl,y], J. Mareš [bc], G.V. Margagliotti [x], A. Margotti [cu], A. Marín [cm], C. Markert [dg], M. Marquard [av], I. Martashvili [dn], N.A. Martin [cm], P. Martinengo [ah], M.I. Martínez [b], G. Martínez García [dc], J. Martin Blanco [dc], Y. Martynov [c], A. Mas [dc], S. Masciocchi [cm], M. Masera [y], A. Masoni [cv], L. Massacrier [dc], A. Mastroserio [ae], A. Matyja [df], C. Mayer [df], J. Mazer [dn], M.A. Mazzoni [cy], F. Meddi [v], A. Menchaca-Rocha [bg], J. Mercado Pérez [ci], M. Meres [aj], Y. Miake [dp], K. Mikhaylov [bi,ba], L. Milano [ah], J. Milosevic [u,v], A. Mischke [az], A.N. Mishra [as], D. Miśkowiec [cm], J. Mitra [dt], C.M. Mitu [be], J. Mlynarz [dw], N. Mohammadi [az], B. Mohanty [bu,dt], L. Molnar [ax], L. Montaño Zetina [k], E. Montes [j], M. Morando [ab], D.A. Moreira De Godoy [di], S. Moretto [ab], A. Morreale [dl], A. Morsch [ah], V. Muccifora [bn], E. Mudnic [de], D. Mühlheim [aw], S. Muhuri [dt], M. Mukherjee [dt], H. Müller [ah], M.G. Munhoz [di], S. Murray [ce], L. Musa [ah], J. Musinsky [bb], B.K. Nandi [ar], R. Nania [cu], E. Nappi [ct], C. Nattrass [dn], K. Nayak [bu], T.K. Nayak [dt], S. Nazarenko [co], A. Nedosekin [ba], M. Nicassio [cm], M. Niculescu [ah,be], B.S. Nielsen [bv], S. Nikolaev [cp], S. Nikulin [cp], V. Nikulin [ca], B.S. Nilsen [cb], F. Noferini [l,cu], P. Nomokonov [bi], G. Nooren [az], A. Nyanin [cp], J. Nystrand [q], H. Oeschler [ci], S. Oh [dy], S.K. Oh [an,vi], A. Okatan [bk], L. Olah [dx], J. Oleniacz [dv], A.C. Oliveira Da Silva [di], J. Onderwaater [cm], C. Oppedisano [da], A. Ortiz Velasquez [af], A. Oskarsson [af], J. Otwinowski [cm], K. Oyama [ci], P. Sahoo [as], Y. Pachmayer [ci], M. Pachr [ak], P. Pagano [ac], G. Paić [bf], F. Painke [am], C. Pajares [p], S.K. Pal [dt], A. Palmeri [cw], D. Pant [ar], V. Papikyan [a], G.S. Pappalardo [cw], P. Pareek [as], W.J. Park [cm], S. Parmar [cc], A. Passfeld [aw], D.I. Patalakha [db], V. Paticchio [ct], B. Paul [cq], T. Pawlak [dv], T. Peitzmann [az], H. Pereira Da Costa [n], E. Pereira De Oliveira Filho [di], D. Peresunko [cp], C.E. Pérez Lara [bw], A. Pesci [cu], V. Peskov [av], Y. Pestov [e], V. Petráček [ak], M. Petran [ak], M. Petris [bt], M. Petrovici [bt], C. Petta [aa], S. Piano [cz], M. Pikna [aj], P. Pillot [dc], O. Pinazza [cu,ah], L. Pinsky [dk], D.B. Piyarathna [dk], M. Płoskoń [bp], M. Planinic [dq,cn], J. Pluta [dv], S. Pochybova [dx], P.L.M. Podesta-Lerma [dh], M.G. Poghosyan [ah], E.H.O. Pohjoisaho [ap], B. Polichtchouk [db], N. Poljak [cn], A. Pop [bt], S. Porteboeuf-Houssais [bl], J. Porter [bp], B. Potukuchi [cf], S.K. Prasad [dw], R. Preghenella [cu,l], F. Prino [da], C.A. Pruneau [dw], I. Pshenichnov [ay], G. Puddu [w], P. Pujahari [dw], V. Punin [co], J. Putschke [dw], H. Qvigstad [u], A. Rachevski [cz], S. Raha [d], J. Rak [dl], A. Rakotozafindrabe [n], L. Ramello [ad], R. Raniwala [cg], S. Raniwala [cg], S.S. Räsänen [ap], B.T. Rascanu [av], D. Rathee [cc], A.W. Rauf [o], V. Razazi [w], K.F. Read [dn], J.S. Real [bm], K. Redlich [bs,vii], R.J. Reed [dy], A. Rehman [q], P. Reichelt [av], M. Reicher [az], F. Reidt [ah], R. Renfordt [av], A.R. Reolon [bn], A. Reshetin [ay], F. Rettig [am], J.-P. Revol [ah], K. Reygers [ci], V. Riabov [ca], R.A. Ricci [bo], T. Richert [af], M. Richter [u], P. Riedler [ah], W. Riegler [ah], F. Riggi [aa], A. Rivetti [da], E. Rocco [az], M. Rodríguez Cahuantzi [b], A. Rodriguez Manso [bw], K. Røed [u], E. Rogochaya [bi], S. Rohni [cf], D. Rohr [am],

D. Röhrich [q], R. Romita [bx], F. Ronchetti [bn], P. Rosnet [bl], A. Rossi [ah], F. Roukoutakis [cd], A. Roy [as], C. Roy [ax], P. Roy [cq], A.J. Rubio Montero [j], R. Rui [x], R. Russo [y], E. Ryabinkin [cp], Y. Ryabov [ca], A. Rybicki [df], S. Sadovsky [db], K. Šafařík [ah], B. Sahlmuller [av], R. Sahoo [as], P.K. Sahu [bd], J. Saini [dt], S. Sakai [bp], C.A. Salgado [p], J. Salzwedel [s], S. Sambyal [cf], V. Samsonov [ca], X. Sanchez Castro [ax], F.J. Sánchez Rodríguez [dh], L. Šándor [bb], A. Sandoval [bg], M. Sano [dp], G. Santagati [aa], D. Sarkar [dt], E. Scapparone [cu], F. Scarlassara [ab], R.P. Scharenberg [ck], C. Schiaua [bt], R. Schicker [ci], C. Schmidt [cm], H.R. Schmidt [ag], S. Schuchmann [av], J. Schukraft [ah], M. Schulc [ak], T. Schuster [dy], Y. Schutz [dc,ah], K. Schwarz [cm], K. Schweda [cm], G. Scioli [z], E. Scomparin [da], R. Scott [dn], G. Segato [ab], J.E. Seger [cb], Y. Sekiguchi [do], I. Selyuzhenkov [cm], J. Seo [cl], E. Serradilla [j,bg], A. Sevcenco [be], A. Shabetai [dc], G. Shabratova [bi], R. Shahoyan [ah], A. Shangaraev [db], N. Sharma [dn], S. Sharma [cf], K. Shigaki [aq], K. Shtejer [y], Y. Sibiriak [cp], S. Siddhanta [cv], T. Siemiarczuk [bs], D. Silvermyr [bz], C. Silvestre [bm], G. Simatovic [dq], R. Singaraju [dt], R. Singh [cf], S. Singha [dt,bu], V. Singhal [dt], B.C. Sinha [dt], T. Sinha [cq], B. Sitar [aj], M. Sitta [ad], T.B. Skaali [u], K. Skjerdal [q], M. Slupecki [dl], N. Smirnov [dy], R.J.M. Snellings [az], C. Søgaard [af], R. Soltz [bq], J. Song [cl], M. Song [dz], F. Soramel [ab], S. Sorensen [dn], M. Spacek [ak], I. Sputowska [df], M. Spyropoulou-Stassinaki [cd], B.K. Srivastava [ck], J. Stachel [ci], I. Stan [be], G. Stefanek [bs], M. Steinpreis [s], E. Stenlund [af], G. Steyn [bh], J.H. Stiller [ci], D. Stocco [dc], M. Stolpovskiy [db], P. Strmen [aj], A.A.P. Suaide [di], T. Sugitate [aq], C. Suire [at], M. Suleymanov [o], R. Sultanov [ba], M. Šumbera [by], T. Susa [cn], T.J.M. Symons [bp], A. Szabo [aj], A. Szanto de Toledo [di], I. Szarka [aj], A. Szczepankiewicz [ah], M. Szymanski [dv], J. Takahashi [dj], M.A. Tangaro [ae], J.D. Tapia Takaki [i,at,viii], A. Tarantola Peloni [av], A. Tarazona Martinez [ah], M.G. Tarzila [bt], A. Tauro [ah], G. Tejeda Muñoz [b], A. Telesca [ah], C. Terrevoli [w], J. Thäder [cm], D. Thomas [az], R. Tieulent [dr], A.R. Timmins [dk], A. Toia [cx], H. Torii [do], V. Trubnikov [c], W.H. Trzaska [dl], T. Tsuji [do], A. Tumkin [co], R. Turrisi [cx], T.S. Tveter [u], J. Ulery [av], K. Ullaland [q], A. Uras [dr], G.L. Usai [w], M. Vajzer [by], M. Vala [bb,bi], L. Valencia Palomo [bl,at], S. Vallero [ci], P. Vande Vyvre [ah], L. Vannucci [bo], J. Van Der Maarel [az], J.W. Van Hoorne [ah], M. van Leeuwen [az], A. Vargas [b], M. Vargyas [dl], R. Varma [ar], M. Vasileiou [cd], A. Vasiliev [cp], V. Vechernin [ds], M. Veldhoen [az], A. Velure [q], M. Venaruzzo [x,bo], E. Vercellin [y], S. Vergara Limón [b], R. Vernet [h], M. Verweij [dw], L. Vickovic [de], G. Viesti [ab], J. Viinikainen [dl], Z. Vilakazi [bh], O. Villalobos Baillie [cr], A. Vinogradov [cp], L. Vinogradov [ds], Y. Vinogradov [co], T. Virgili [ac], Y.P. Viyogi [dt], A. Vodopyanov [bi], M.A. Völkl [ci], K. Voloshin [ba], S.A. Voloshin [dw], G. Volpe [ah], B. von Haller [ah], I. Vorobyev [ds], D. Vranic [cm,ah], J. Vrláková [al], B. Vulpescu [bl], A. Vyushin [co], B. Wagner [q], J. Wagner [cm], V. Wagner [ak], M. Wang [g,dc], Y. Wang [ci], D. Watanabe [dp], M. Weber [dk], J.P. Wessels [aw], U. Westerhoff [aw], J. Wiechula [ag], J. Wikne [u], M. Wilde [aw], G. Wilk [bs], J. Wilkinson [ci], M.C.S. Williams [cu], B. Windelband [ci], M. Winn [ci], C. Xiang [g], C.G. Yaldo [dw], Y. Yamaguchi [do], H. Yang [az], P. Yang [g], S. Yang [q], S. Yano [aq], S. Yasnopolskiy [cp], J. Yi [cl], Z. Yin [g], I.-K. Yoo [cl], I. Yushmanov [cp], V. Zaccolo [bv], C. Zach [ak], A. Zaman [o], C. Zampolli [cu], S. Zaporozhets [bi], A. Zarochentsev [ds], P. Závada [bc], N. Zaviyalov [co], H. Zbroszczyk [dv], I.S. Zgura [be], M. Zhalov [ca], H. Zhang [g], X. Zhang [bp,g], Y. Zhang [g], C. Zhao [u], N. Zhigareva [ba], D. Zhou [g], F. Zhou [g], Y. Zhou [az], Zhuo Zhou [q], H. Zhu [g], J. Zhu [g], X. Zhu [g], A. Zichichi [l,z], A. Zimmermann [ci], M.B. Zimmermann [ah,aw], G. Zinovjev [c], Y. Zoccarato [dr], M. Zyzak [av]

[a] *A.I. Alikhanyan National Science Laboratory (Yerevan Physics Institute) Foundation, Yerevan, Armenia*
[b] *Benemérita Universidad Autónoma de Puebla, Puebla, Mexico*
[c] *Bogolyubov Institute for Theoretical Physics, Kiev, Ukraine*
[d] *Bose Institute, Department of Physics and Centre for Astroparticle Physics and Space Science (CAPSS), Kolkata, India*
[e] *Budker Institute for Nuclear Physics, Novosibirsk, Russia*
[f] *California Polytechnic State University, San Luis Obispo, CA, United States*
[g] *Central China Normal University, Wuhan, China*
[h] *Centre de Calcul de l'IN2P3, Villeurbanne, France*
[i] *Centro de Aplicaciones Tecnológicas y Desarrollo Nuclear (CEADEN), Havana, Cuba*
[j] *Centro de Investigaciones Energéticas Medioambientales y Tecnológicas (CIEMAT), Madrid, Spain*
[k] *Centro de Investigación y de Estudios Avanzados (CINVESTAV), Mexico City and Mérida, Mexico*
[l] *Centro Fermi – Museo Storico della Fisica e Centro Studi e Ricerche "Enrico Fermi", Rome, Italy*
[m] *Chicago State University, Chicago, United States*
[n] *Commissariat à l'Energie Atomique, IRFU, Saclay, France*
[o] *COMSATS Institute of Information Technology (CIIT), Islamabad, Pakistan*
[p] *Departamento de Física de Partículas and IGFAE, Universidad de Santiago de Compostela, Santiago de Compostela, Spain*
[q] *Department of Physics and Technology, University of Bergen, Bergen, Norway*
[r] *Department of Physics, Aligarh Muslim University, Aligarh, India*
[s] *Department of Physics, Ohio State University, Columbus, OH, United States*
[t] *Department of Physics, Sejong University, Seoul, South Korea*
[u] *Department of Physics, University of Oslo, Oslo, Norway*
[v] *Dipartimento di Fisica dell'Università 'La Sapienza' and Sezione INFN Rome, Italy*
[w] *Dipartimento di Fisica dell'Università and Sezione INFN, Cagliari, Italy*
[x] *Dipartimento di Fisica dell'Università and Sezione INFN, Trieste, Italy*

[y] *Dipartimento di Fisica dell'Università and Sezione INFN, Turin, Italy*
[z] *Dipartimento di Fisica e Astronomia dell'Università and Sezione INFN, Bologna, Italy*
[aa] *Dipartimento di Fisica e Astronomia dell'Università and Sezione INFN, Catania, Italy*
[ab] *Dipartimento di Fisica e Astronomia dell'Università and Sezione INFN, Padova, Italy*
[ac] *Dipartimento di Fisica 'E.R. Caianiello' dell'Università and Gruppo Collegato INFN, Salerno, Italy*
[ad] *Dipartimento di Scienze e Innovazione Tecnologica dell'Università del Piemonte Orientale and Gruppo Collegato INFN, Alessandria, Italy*
[ae] *Dipartimento Interateneo di Fisica 'M. Merlin' and Sezione INFN, Bari, Italy*
[af] *Division of Experimental High Energy Physics, University of Lund, Lund, Sweden*
[ag] *Eberhard Karls Universität Tübingen, Tübingen, Germany*
[ah] *European Organization for Nuclear Research (CERN), Geneva, Switzerland*
[ai] *Faculty of Engineering, Bergen University College, Bergen, Norway*
[aj] *Faculty of Mathematics, Physics and Informatics, Comenius University, Bratislava, Slovakia*
[ak] *Faculty of Nuclear Sciences and Physical Engineering, Czech Technical University in Prague, Prague, Czech Republic*
[al] *Faculty of Science, P.J. Šafárik University, Košice, Slovakia*
[am] *Frankfurt Institute for Advanced Studies, Johann Wolfgang Goethe-Universität Frankfurt, Frankfurt, Germany*
[an] *Gangneung-Wonju National University, Gangneung, South Korea*
[ao] *Gauhati University, Department of Physics, Guwahati, India*
[ap] *Helsinki Institute of Physics (HIP), Helsinki, Finland*
[aq] *Hiroshima University, Hiroshima, Japan*
[ar] *Indian Institute of Technology Bombay (IIT), Mumbai, India*
[as] *Indian Institute of Technology Indore, Indore (IITI), India*
[at] *Institut de Physique Nucléaire d'Orsay (IPNO), Université Paris-Sud, CNRS-IN2P3, Orsay, France*
[au] *Institut für Informatik, Johann Wolfgang Goethe-Universität Frankfurt, Frankfurt, Germany*
[av] *Institut für Kernphysik, Johann Wolfgang Goethe-Universität Frankfurt, Frankfurt, Germany*
[aw] *Institut für Kernphysik, Westfälische Wilhelms-Universität Münster, Münster, Germany*
[ax] *Institut Pluridisciplinaire Hubert Curien (IPHC), Université de Strasbourg, CNRS-IN2P3, Strasbourg, France*
[ay] *Institute for Nuclear Research, Academy of Sciences, Moscow, Russia*
[az] *Institute for Subatomic Physics of Utrecht University, Utrecht, Netherlands*
[ba] *Institute for Theoretical and Experimental Physics, Moscow, Russia*
[bb] *Institute of Experimental Physics, Slovak Academy of Sciences, Košice, Slovakia*
[bc] *Institute of Physics, Academy of Sciences of the Czech Republic, Prague, Czech Republic*
[bd] *Institute of Physics, Bhubaneswar, India*
[be] *Institute of Space Science (ISS), Bucharest, Romania*
[bf] *Instituto de Ciencias Nucleares, Universidad Nacional Autónoma de México, Mexico City, Mexico*
[bg] *Instituto de Física, Universidad Nacional Autónoma de México, Mexico City, Mexico*
[bh] *iThemba LABS, National Research Foundation, Somerset West, South Africa*
[bi] *Joint Institute for Nuclear Research (JINR), Dubna, Russia*
[bj] *Korea Institute of Science and Technology Information, Daejeon, South Korea*
[bk] *KTO Karatay University, Konya, Turkey*
[bl] *Laboratoire de Physique Corpusculaire (LPC), Clermont Université, Université Blaise Pascal, CNRS-IN2P3, Clermont-Ferrand, France*
[bm] *Laboratoire de Physique Subatomique et de Cosmologie, Université Grenoble-Alpes, CNRS-IN2P3, Grenoble, France*
[bn] *Laboratori Nazionali di Frascati, INFN, Frascati, Italy*
[bo] *Laboratori Nazionali di Legnaro, INFN, Legnaro, Italy*
[bp] *Lawrence Berkeley National Laboratory, Berkeley, CA, United States*
[bq] *Lawrence Livermore National Laboratory, Livermore, CA, United States*
[br] *Moscow Engineering Physics Institute, Moscow, Russia*
[bs] *National Centre for Nuclear Studies, Warsaw, Poland*
[bt] *National Institute for Physics and Nuclear Engineering, Bucharest, Romania*
[bu] *National Institute of Science Education and Research, Bhubaneswar, India*
[bv] *Niels Bohr Institute, University of Copenhagen, Copenhagen, Denmark*
[bw] *Nikhef, National Institute for Subatomic Physics, Amsterdam, Netherlands*
[bx] *Nuclear Physics Group, STFC Daresbury Laboratory, Daresbury, United Kingdom*
[by] *Nuclear Physics Institute, Academy of Sciences of the Czech Republic, Řež u Prahy, Czech Republic*
[bz] *Oak Ridge National Laboratory, Oak Ridge, TN, United States*
[ca] *Petersburg Nuclear Physics Institute, Gatchina, Russia*
[cb] *Physics Department, Creighton University, Omaha, NE, United States*
[cc] *Physics Department, Panjab University, Chandigarh, India*
[cd] *Physics Department, University of Athens, Athens, Greece*
[ce] *Physics Department, University of Cape Town, Cape Town, South Africa*
[cf] *Physics Department, University of Jammu, Jammu, India*
[cg] *Physics Department, University of Rajasthan, Jaipur, India*
[ch] *Physik Department, Technische Universität München, Munich, Germany*
[ci] *Physikalisches Institut, Ruprecht-Karls-Universität Heidelberg, Heidelberg, Germany*
[cj] *Politecnico di Torino, Turin, Italy*
[ck] *Purdue University, West Lafayette, IN, United States*
[cl] *Pusan National University, Pusan, South Korea*
[cm] *Research Division and ExtreMe Matter Institute EMMI, GSI Helmholtzzentrum für Schwerionenforschung, Darmstadt, Germany*
[cn] *Rudjer Bošković Institute, Zagreb, Croatia*
[co] *Russian Federal Nuclear Center (VNIIEF), Sarov, Russia*
[cp] *Russian Research Centre Kurchatov Institute, Moscow, Russia*
[cq] *Saha Institute of Nuclear Physics, Kolkata, India*
[cr] *School of Physics and Astronomy, University of Birmingham, Birmingham, United Kingdom*
[cs] *Sección Física, Departamento de Ciencias, Pontificia Universidad Católica del Perú, Lima, Peru*
[ct] *Sezione INFN, Bari, Italy*
[cu] *Sezione INFN, Bologna, Italy*
[cv] *Sezione INFN, Cagliari, Italy*
[cw] *Sezione INFN, Catania, Italy*
[cx] *Sezione INFN, Padova, Italy*
[cy] *Sezione INFN, Rome, Italy*

cz *Sezione INFN, Trieste, Italy*
da *Sezione INFN, Turin, Italy*
db *SSC IHEP of NRC Kurchatov Institute, Protvino, Russia*
dc *SUBATECH, Ecole des Mines de Nantes, Université de Nantes, CNRS-IN2P3, Nantes, France*
dd *Suranaree University of Technology, Nakhon Ratchasima, Thailand*
de *Technical University of Split FESB, Split, Croatia*
df *The Henryk Niewodniczanski Institute of Nuclear Physics, Polish Academy of Sciences, Cracow, Poland*
dg *The University of Texas at Austin, Physics Department, Austin, TX, United States*
dh *Universidad Autónoma de Sinaloa, Culiacán, Mexico*
di *Universidade de São Paulo (USP), São Paulo, Brazil*
dj *Universidade Estadual de Campinas (UNICAMP), Campinas, Brazil*
dk *University of Houston, Houston, TX, United States*
dl *University of Jyväskylä, Jyväskylä, Finland*
dm *University of Liverpool, Liverpool, United Kingdom*
dn *University of Tennessee, Knoxville, TN, United States*
do *University of Tokyo, Tokyo, Japan*
dp *University of Tsukuba, Tsukuba, Japan*
dq *University of Zagreb, Zagreb, Croatia*
dr *Université de Lyon, Université Lyon 1, CNRS/IN2P3, IPN-Lyon, Villeurbanne, France*
ds *V. Fock Institute for Physics, St. Petersburg State University, St. Petersburg, Russia*
dt *Variable Energy Cyclotron Centre, Kolkata, India*
du *Vestfold University College, Tonsberg, Norway*
dv *Warsaw University of Technology, Warsaw, Poland*
dw *Wayne State University, Detroit, MI, United States*
dx *Wigner Research Centre for Physics, Hungarian Academy of Sciences, Budapest, Hungary*
dy *Yale University, New Haven, CT, United States*
dz *Yonsei University, Seoul, South Korea*
ea *Zentrum für Technologietransfer und Telekommunikation (ZTT), Fachhochschule Worms, Worms, Germany*

  i Also at: St. Petersburg State Polytechnical University.
 ii Deceased.
iii Also at: Department of Applied Physics, Aligarh Muslim University, Aligarh, India.
 iv Also at: M.V. Lomonosov Moscow State University, D.V. Skobeltsyn Institute of Nuclear Physics, Moscow, Russia.
  v Also at: University of Belgrade, Faculty of Physics and "Vinča" Institute of Nuclear Sciences, Belgrade, Serbia.
 vi Permanent Address: Konkuk University, Seoul, South Korea.
vii Also at: Institute of Theoretical Physics, University of Wroclaw, Wroclaw, Poland.
viii Also at: University of Kansas, Lawrence, KS, United States.